



Incommensurate SDW in cuprates

G. Nikšić*, I. Kupčić, D.K. Sunko, S. Barišić

Department of Physics, Faculty of Science, University of Zagreb, Bijenička 32, 10000 Zagreb, Croatia

ARTICLE INFO

Available online 9 January 2012

Keywords:

High T_c
Cuprates
Antiferromagnetism
Pseudogap
Neutron scattering

ABSTRACT

The incommensurate antiferromagnetism (AF) in metallic underdoped cuprates is interpreted with several complementary approaches, unified by a consistent disambiguation of the copper and oxygen degrees of freedom. Collinear (with respect to the copper lattice) peaks in the neutron response at low frequency are due to the oxygen-dominated arcs, while the diagonal peaks at high frequency or low doping come from the copper-dominated vH points. The latter switch from collinear to diagonal as the frequency increases. The direct O–O overlap induces an AF which is weaker and thermodynamically preferred to the AF of strongly localized copper sites, and which coexists with Fermi arcs. A theoretical understanding of the strongly \mathbf{k} -dependent AF gap observed in ARPES and STM measurements is proposed.

© 2012 Elsevier B.V. All rights reserved.

1. Introduction

The nature of the pseudogap phase (PG) and its relation to the antiferromagnetic (AF) and superconducting (SC) phases in cuprates remains one of the most intriguing open topics in condensed matter physics, despite the experimental advances and numerous theoretical models in the last 25 years. It is now clear from angle-resolved photoemission [1] (ARPES) and tunneling microscopy [2] (STM) measurements that both PG and SC gaps are large near the vH points and small near the BZ diagonal, but with a different shape (similar to the letters U and V, respectively, as one follows the Fermi surface) and temperature dependence.

Recent microwave measurements [3] have shown that superconducting fluctuations appear in a much smaller temperature range than $T^* - T_c$, meaning that the PG phase cannot be attributed to SC fluctuations alone in the metallic underdoped ($T_c < T < T^*$) part of the phase diagram. Neutron scattering experiments show incommensurate (IC) peaks near the AF wave vector. The orientation and location of these signals evolve with doping and frequency [4,5]. The distance of the peaks from the AF wave vector is linear in doping, but the change with frequency exhibits several behaviors in different compound families.

2. Model

We start with a system near half filling whose electronic states are described with a three-band dispersion in the “anticrossing” regime, with significant oxygen–oxygen hopping t_{pp} , so that the

effective copper level intersects the bare oxygen band. The open band is conveniently modeled with a $t-t'$ dispersion, with the understanding that the physical reason for the Fermi surface curvatures induced by the t' term is strong particle–hole (ph) symmetry breaking, due to the oxygen levels in real systems [6,7].

We proceed with modeling in two steps. First, the crossover at T^* is modeled as a genuine phase transition, here induced by a strongly repulsive effective Hubbard interaction U_{eff} between two holes of opposite spins on the same site in the Hubbard Hamiltonian in Eq. (1). Notably, this U_{eff} is not a bare Coulomb U -term, as explained more fully below. We introduce an effective mean-field (MF) Hamiltonian, Eq. (2), keeping only the $\mathbf{Q} = (\pi, \pi)$ part. This effective Hamiltonian is presented here in the usual l, \mathbf{k} representation, where $l = \pm 1$ indices represent the \mathbf{k} and $\mathbf{k} - \mathbf{Q}$ states, respectively. This MF Hamiltonian can be diagonalized with a 2×2 spin dependent transformation $U_{\mathbf{k}, \sigma}(\pm, \pm)$, to obtain two zeroth-order bands E_{\pm} , given in Eq. (3). The gap between the bands, proportional to U_{eff} and the average spin per site, should be calculated self-consistently. The chemical potential cuts across both bands, producing the well-known image of oval pockets around the zone diagonal (arcs) from one band, and squarish pockets around the vH point from the other. By comparison with the three-band model in the anticrossing regime, we identify the arcs as oxygen (O)-dominated and vH pockets as copper (Cu)-dominated. These physical designations will be used from now on. In the second step, we fill the zeroth-order gap with ph excitations, to recover the pseudogap at low temperature. The zeroth-order model reads

$$H = \sum_{\mathbf{k}\sigma} \varepsilon_{\mathbf{k}} a_{\mathbf{k}\sigma}^{\dagger} a_{\mathbf{k}\sigma} + U_{\text{eff}} \sum_n n_{n\uparrow} n_{n\downarrow} \quad (1)$$

$$H_{\text{MF}} = \sum_{\|k_x > 0\sigma} H^{ll'}(\mathbf{k}, \sigma) a_{\mathbf{k}\sigma}^{\dagger} a_{l'\mathbf{k}\sigma} \quad (2)$$

* Corresponding author. Tel.: +385 1 460 5563; fax: +385 1 468 0 336.
E-mail address: gnksic@phy.hr (G. Nikšić).

$$H^{++} = \varepsilon_{\mathbf{k}}, \quad H^{+-} = -2\Delta\sigma$$

$$H^{-+} = 2\Delta\sigma, \quad H^{--} = \varepsilon_{\mathbf{k}-\mathbf{Q}}$$

$$E_{\pm}(\mathbf{k}) = \frac{\varepsilon_{\mathbf{k}} + \varepsilon_{\mathbf{k}-\mathbf{Q}}}{2} \pm \sqrt{\left(\frac{\varepsilon_{\mathbf{k}} - \varepsilon_{\mathbf{k}-\mathbf{Q}}}{2}\right)^2 + 4\Delta^2} \quad (3)$$

As to the first step, there have been varying approaches to the gap function in the literature. Initially, a constant (“s-wave”) gap on a simple square lattice was considered, through the mean-field Hamiltonian as above, under the assumption of a constant interaction U , associated with the on-site repulsion on the coppers [8]. This procedure produces the constant-gap dispersions in Eq. (3). Subsequent approaches tended to include the superconducting (SC) gap as well, while allowing for a deformed Fermi surface in accord with ARPES data [9,10]. Our program is to describe the physics above T_c with an anisotropic pseudogap as far as possible without including SG.

Recent precise measurements of the gap function at the Fermi level in underdoped cuprates above T_c allow us to put its experimentally observed form in the gapped dispersions E_{\pm} . It is not an s -wave, or a d -wave either, but more like a step function, with a large gap at the vH points and no gap on the nodal arc. For our purposes the empirical form

$$\Delta_f = \frac{\Delta_0}{32} (\cos k_x - \cos k_y)^5 \quad (4)$$

was found adequately close to the measured one, so we generalize the mean field approach by assuming a \mathbf{k} -dependent gap function, without self-consistency, which will be addressed in the following sections. In this paper we use a dispersion of carrier states on a square lattice with second-nearest neighbor hoppings and a ratio of $t'/t = -0.25$ and gap magnitude of $\Delta_0 = 0.1t$, unless indicated otherwise.

Whichever gap function is chosen, s , d , or Eq. (4), it produces broadly similar bands in the first step. There appear new saddle-point singularities at incommensurate \mathbf{k} -points in the zone near the old vH points, with a logarithmic density of states (DOS). This is welcome in light of neutron scattering experiments which clearly see an incommensurate response, of which a large part is now modeled as the bare DOS of the split bands. However, it also indicates that the first step is not self-consistent, because the assumed commensurate AF instability gives an incommensurate outcome already in zeroth order.

The real test of the approach is in the second step, when the ph responses are calculated, and compared with experiment. The bare susceptibilities represent a particle–hole pair of a definite spin configuration in either of the initial and final states \mathbf{q} , $\mathbf{q} + \mathbf{Q}$, mixed with an AF potential. We will focus here on the transversal spin susceptibility χ_{+-} as it was shown [11] that its contribution to the Pauli-like susceptibility is dominant. When all different combinations of incoming and outgoing values of \mathbf{q} are accounted for, χ_0 becomes a 2×2 matrix, with elements shown in Fig. 1.

Each of the propagators in Fig. 1 can be expressed as a projection on the two magnetic bands

$$\mathcal{G}_{\sigma\sigma'}^{ll'}(\mathbf{k}, i\omega_n) = \sum_{L=\pm} U_{\mathbf{k}\sigma}(l, L) U_{\mathbf{k}\sigma'}^*(l', L) \mathcal{G}_{\sigma\sigma'}^{LL}(\mathbf{k}, i\omega_n)$$

In the next section, we show the four inter- and intraband contributions for the transversal spin channel and compare with neutron experiments.

3. Results

Eq. (4) is noticeably superior to the s and d -wave AF gap in reproducing the qualitative behavior found in experiment. In

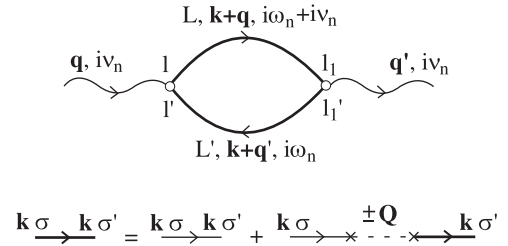


Fig. 1. The bare susceptibility matrix (top). Due to the SDW potential, each fermion line can exit the diagram with a momentum shift of $\pm \mathbf{Q}$, so the fermion lines are a solution of the mean-field SDW (AF) Dyson equation (bottom) which produces the two SDW (AF) bands. Thus there are four distinct combinations of states $l, l' = \pm$ and corresponding momenta \mathbf{q}, \mathbf{q}' : the initial and final momentum can be either \mathbf{q} or $\mathbf{q} \pm \mathbf{Q}$.

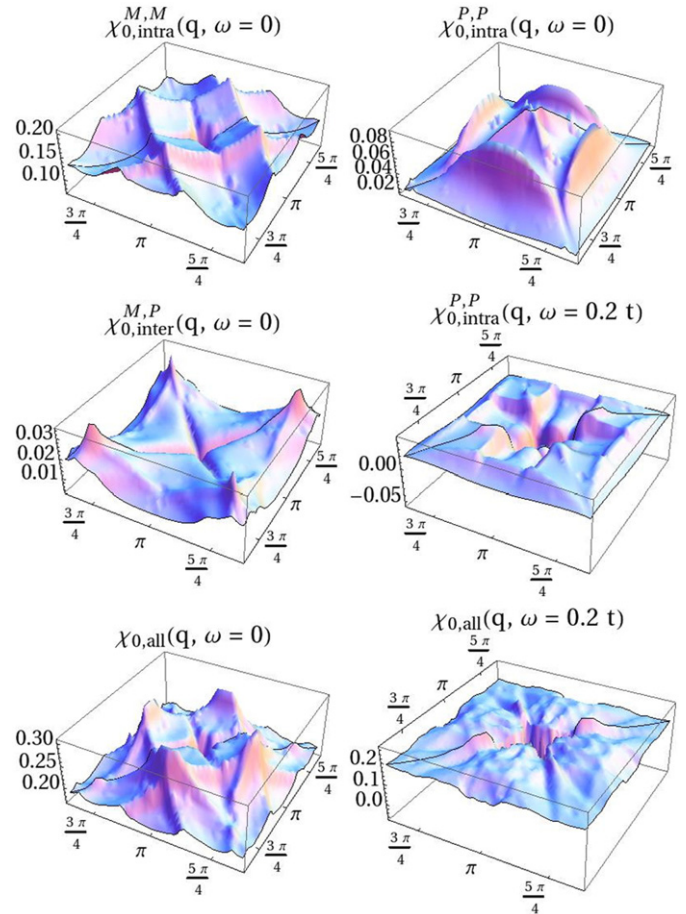


Fig. 2. Total and partial bare susceptibilities $\chi_{\uparrow\downarrow}^0$, at $\omega=0$ (left) and $\omega=0.2t$ (right). M : arcs (E_{-} , O), P : vH (E_{+} , Cu).

Fig. 2. O-dominated arcs have collinear peaks in their intraband susceptibility, while the Cu-dominated vH pockets change their intraband response with frequency: at low frequency they are collinear, while at higher frequency they switch to diagonal. The peaks in the interband Cu–O response are diagonal, but much weaker and further away from the AF point than the intraband peaks, so we do not consider them relevant at present for the experimental comparison. Significantly, the zero frequency responses in both Cu and O channels conspire to produce the collinear peaks observed in experiment. The switch to diagonal peaks at high frequency is essentially Cu-driven, because the O channel only becomes featureless.

To put these observations in perspective, we recall that the $t-t'$ dispersion is but a stand-in for the physical three-band dispersion, which has proven most efficient in parametrizing ARPES data [12]. Thus we do not expect too much of it quantitatively, but find it encouraging that it already allows a classification of experimental responses in clear-cut physical terms. This clarity is mainly due to our taking the experimental U-shaped AF gap seriously, which begs the question, how it can be understood theoretically. We hope the physical \mathbf{k} -dependent vertex, identified in the next section, will enable us to justify the observed AF gap shape in a future complete self-consistent calculation.

In the meanwhile, we have checked the effect of local ph symmetry breaking by adding a t' term to the simplest self-consistent calculation (Eq. (5)) with an s -wave gap [8]. However, we do not interpret the repulsive on-site interaction there as a bare Hubbard U term, but as a strongly renormalized effective repulsion U_{eff} , essentially the constant part of the same vertex which should be responsible for the observed U-shaped gap. As shown in Fig. 3, the t' term induces a qualitative change in the solution of the gap equation

$$\frac{1}{U_{\text{eff}}} = \sum_{\mathbf{k}}^* \frac{f_{P\uparrow}(\mathbf{k}) - f_{M\downarrow}(\mathbf{k})}{\sqrt{(\varepsilon_{\mathbf{k}} - \varepsilon_{\mathbf{k}-\mathbf{Q}})^2 + \Delta^2}} \quad (5)$$

For certain values of U_{eff} , there now appear two solutions to the AF gap equation, one which reduces to the “old” solution with $t' = 0$ [8], and a new one with much smaller self-consistent gap Δ . We call them the strong and weak gap, respectively. The weak gap is thermodynamically preferred whenever it appears. At half-filling, the difference between them is physically most transparent: while the strong gap is so large that it predicts an AF insulator, the weak gap separates the bands much less, so it already opens the Fermi arcs. Thus we associate the weakening of antiferromagnetism with the appearance of the delocalized oxygen-dominated states in the arcs, which are primarily responsible for conduction in the PG state.

If U_{eff} is large, only the strong gap appears, while if it is too small, there is no solution. The peak and the associated weak solution to the left of it appear only when $t' \neq 0$, while for $t' = 0$ there is an arbitrarily small gap at half-filling for arbitrarily small U_{eff} , as shown by the dashed curve. Such behavior is clearly an artefact of ph symmetry, absent in real high- T_c cuprates.

The complete phase diagram is shown in Fig. 4. The “kink” in the red curves, delimiting the weak-gap solution, is at the vH filling, so the underdoped region is to its left. If U_{eff} is between the

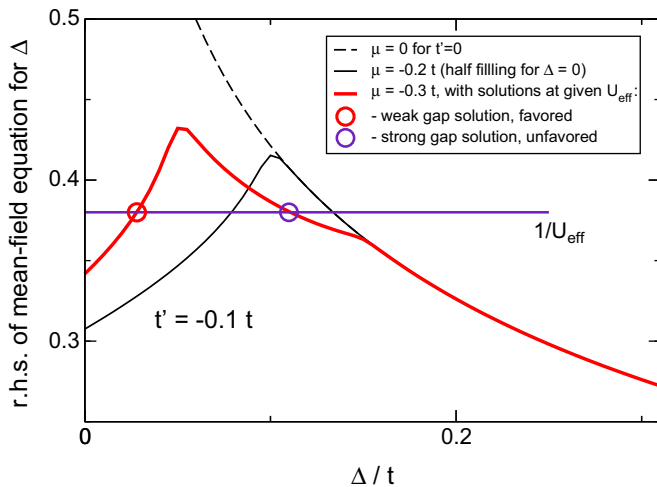


Fig. 3. The effect of ph symmetry breaking on the self-consistent calculation of the AF gap. Dotted line: $t' = 0$, Ref. [8].

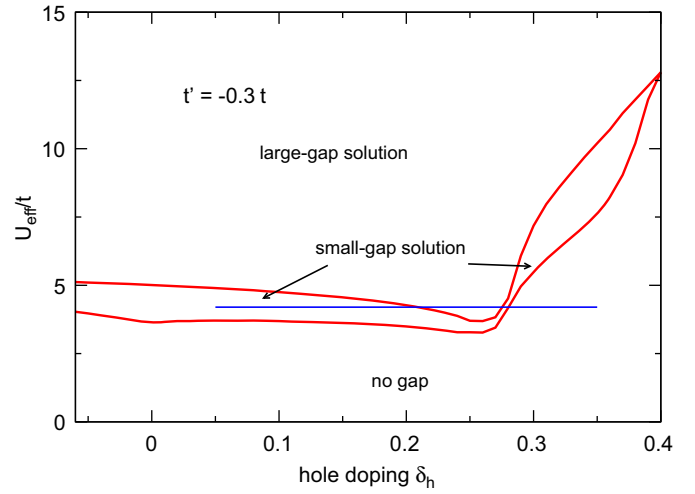


Fig. 4. Phase diagram of the solutions shown in Fig. 3. Horizontal line: an interesting choice of U_{eff} . (For interpretation of the references to color in this figure legend, the reader is referred to the web version of this article.)

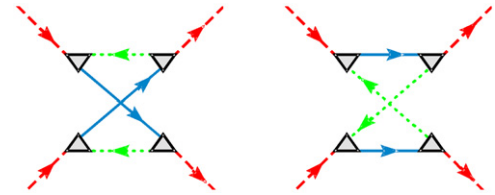


Fig. 5. Scattering of non-interacting Cu–O hybridized fermions on intermittently occupied strongly correlated copper sites [13]. Red lines are holes in the oxygen bands. They hybridize with the copper states, here represented in the slave-fermion formalism: full lines are slave-bosons with spin 1/2, and dotted lines are spinless slave-fermions on the copper sites. (For interpretation of the references to color in this figure legend, the reader is referred to the web version of this article.)

limit curves there, obviously the gap will disappear beyond optimal doping, a physically sensible behavior. A striking feature is the possibility of reappearance of strong magnetism near optimal doping, shortly before it disappears, as observed by following the horizontal line. (Note that a self-consistent U_{eff} should increase at very low doping.) Given the crude, one-parameter $t-t'$ dispersion, we plan to reproduce this diagram in a three-band setting in order to compare it quantitatively with real materials. However, we believe its qualitative features will persevere, at least for dopings in the metallic region.

4. Theoretical basis

The above physical interpretations of the observed neutron scattering data are based on the phenomenological input of the observed, strongly U-shaped AF gap which opens at T^* . In Fig. 5, we show the lowest order of the corresponding scattering vertex, as proposed in a perturbation theory based on a slave-fermion decomposition of the Cu d -electrons [13]. The physical process depicted by the diagrams is that a zeroth-order Cu–O hybridized non-interacting hole in a wide band in \mathbf{k} -space arrives at each unit cell via the oxygen sites. In order to stay Cu–O hybridized, the hole has to visit the copper site via an overlap t_{pd} , but to do this it has to wait until the copper is empty of other holes, of either spin. This gives rise to the scattering in the internal part of the diagram, where spinless slave-fermions are depicted by dotted, and slave bosons by full lines. The vertex is associated with a strong \mathbf{k} -dependence essentially from projecting the

itinerant holes onto the localized coppers, because the latter dominate the Fermi surface states near the vH points.

Analogous vertices can be constructed with *d*-electrons (slave-particle bubbles) on the external lines. This opens the way for a complete self-consistent theory of magnetism in the three-band model. We hope to show it can reproduce the observed U-shaped AF gap.

5. Conclusions

We have presented several complementary inroads to the problem of magnetic responses in the cuprates in the PG region of the phase diagram. They converge to the interpretation that the PG physics is significantly different from the one suggested by a *ph*-symmetric view of the copper sites. The breaking of *ph* symmetry induced by the presence of oxygens in real materials gives rise to an AF gap with a much stronger **k**-dependence than the SC gap. The physical bridging of the strongly correlated copper sites by the uncorrelated oxygens opens a channel for the renormalization of the strong interactions, simply by their avoidance through the O–O overlap. The same overlap destabilizes the

AF of the localized copper sites and replaces it by a much weaker, qualitatively different AF, which can coexist with the itinerancy of the oxygen-dominated Fermi arcs. We are working to corroborate these results in the more sophisticated setting of the three-band model with realistic, self-consistent effective interactions.

References

- [1] W.S. Lee, et al., Nature 450 (2007) 81.
- [2] M.C. Boyer, et al., Nature Phys. 3 (2007) 802.
- [3] M.S. Grbić, et al., Phys. Rev. B 83 (2011) 144508.
- [4] D. Reznik, et al., Phys. Rev. Lett. 93 (2004) 207003.
- [5] S.R. Dunsiger, et al., Phys. Rev. B 78 (2008) 092507.
- [6] Q. Si, et al., Phys. Rev. B 47 (1993) 9055.
- [7] G. Nikšić, O.S. Barišić, I. Kupčić, D.K. Sunko, S. Barišić, Physica B, doi:10.1016/j.physb.2012.01.042, this issue.
- [8] J.R. Schrieffer, et al., Phys. Rev. B 39 (1989) 11663.
- [9] Y.-J. Kao, et al., Phys. Rev. B 61 (2000) R11898.
- [10] M.R. Norman, Phys. Rev. B 63 (2001) 092509.
- [11] A.V. Chubukov, D.M. Frenkel, Phys. Rev. B 46 (1992) 11884.
- [12] D.K. Sunko, S. Barišić, Eur. Phys. J. B 46 (2005) 269; D.K. Sunko, S. Barišić, Phys. Rev. B 75 (2007) 060506. (R).
- [13] S. Barišić, O.S. Barišić, Phys. B: Condens. Matter 404 (2009) 370. preprint arXiv:1110.1947.